

Long-range energy transfer in proteins

Francesco Piazza

*Ecole Polytechnique Fédérale de Lausanne, Laboratoire de Biophysique Statistique,
ITP-SB, BSP-720, CH-1015 Lausanne, Switzerland and
Centre Européen de Calcul Atomique et Moléculaire (CECAM),
SB CECAM-GE, PPH 335 station 13, CH-1015 Lausanne, Switzerland.*

Yves-Henri Sanejouand

*Laboratoire Biotechnologie, Biocatalyse et Biorégulation,
UMR 6204 du CNRS, Faculté des Sciences et des Techniques,
2, rue de la Houssinière, 44322 Nantes Cedex 3, France.*

Proteins are large and complex molecular machines. In order to perform their function, most of them need energy, *e.g.* either in the form of a photon, like in the case of the visual pigment rhodopsin, or through the breaking of a chemical bond, as in the presence of adenosine triphosphate (ATP). Such energy, in turn, has to be transmitted to specific locations, often several tens of Å away from where it is initially released. Here we show, within the framework of a coarse-grained nonlinear network model, that energy in a protein can jump from site to site with high yields, covering in many instances remarkably large distances. Following single-site excitations, few specific sites are targeted, systematically within the stiffest regions. Such energy transfers mark the spontaneous formation of a localized mode of nonlinear origin at the destination site, which acts as an efficient energy-accumulating centre. Interestingly, yields are found to be optimum for excitation energies in the range of biologically relevant ones.

PACS numbers: 87.14.E-, 63.20.Pw, 87.15.A-

Keywords: Nonlinearity, Energy transfer, Discrete Breathers, Nonlinear Network Model, Enzymes.

Protein dynamics is encoded in their structures and is often critical for their function [2]. Since the early eighties, it is well known that vibrational non-harmonicity has to be accounted for to understand intra-structure energy redistribution [3, 4, 5, 6, 7, 8]. Among nonlinear effects, localized modes were suggested to play a key role [9, 10, 11], including topological excitations, such as solitons [12, 13] as well as Discrete Breathers (DB) [14, 15]. The latter, also known as intrinsic localized modes (ILMs), are spatially localized, time-periodic vibrations found generically in many systems as a combined effect of nonlinearity and spatial discreteness [16, 17]. Notably, DBs are able to *harvest* from the background and pin down for long times amounts of energy much larger than $k_B T$. Indeed, their ability to pump energy from neighboring sites is a distinctive signature of DB self-excitation [18], *e.g.* observed as a consequence of surface cooling [19, 20, 21, 22] or due to modulational instability of band-edge waves in nonlinear lattices [23, 24]. Therefore, provided such phenomena are compatible with cellular constraints, it is tempting to speculate that evolution has found a way to put such long-lived modes at work for lowering energy barriers associated with chemical reactions, *e.g.* for boosting enzyme efficiency during catalytic processes [25].

I. NONLINEAR NETWORK MODEL

Recently, within the framework of a coarse-grained nonlinear network model (NNM), we have shown that DBs in proteins feature strongly site-modulated properties [1, 19]. More precisely, we have shown that spatially localized band-edge Normal Modes (NM) can be continued from low energies to DB solutions centered at the same sites as the corresponding NMs (the NM sites). Note that the latter lie, as a rule, within the stiffest regions of a protein [1, 19]. More generally, however, DBs display a gap in their excitation spectrum. As a consequence, they can “jump” to another site as their energy is varied, following spatial selection rules matching the pattern of DBs localized elsewhere [1]. As a matter of fact, such jumps realize efficient *energy transfers*. Hereafter, we show that events of this kind, connecting with high yields even widely separated locations, can be triggered by a localized excitation, so long as its energy E_0 lies above a given threshold.

II. RESULTS

A. Discrete Breather Excitation

Fig. 1 summarizes the outcome of one such experiment, where energy is initially either localized in NM (M) or in real (R) space. Typically, the initial excitation is found

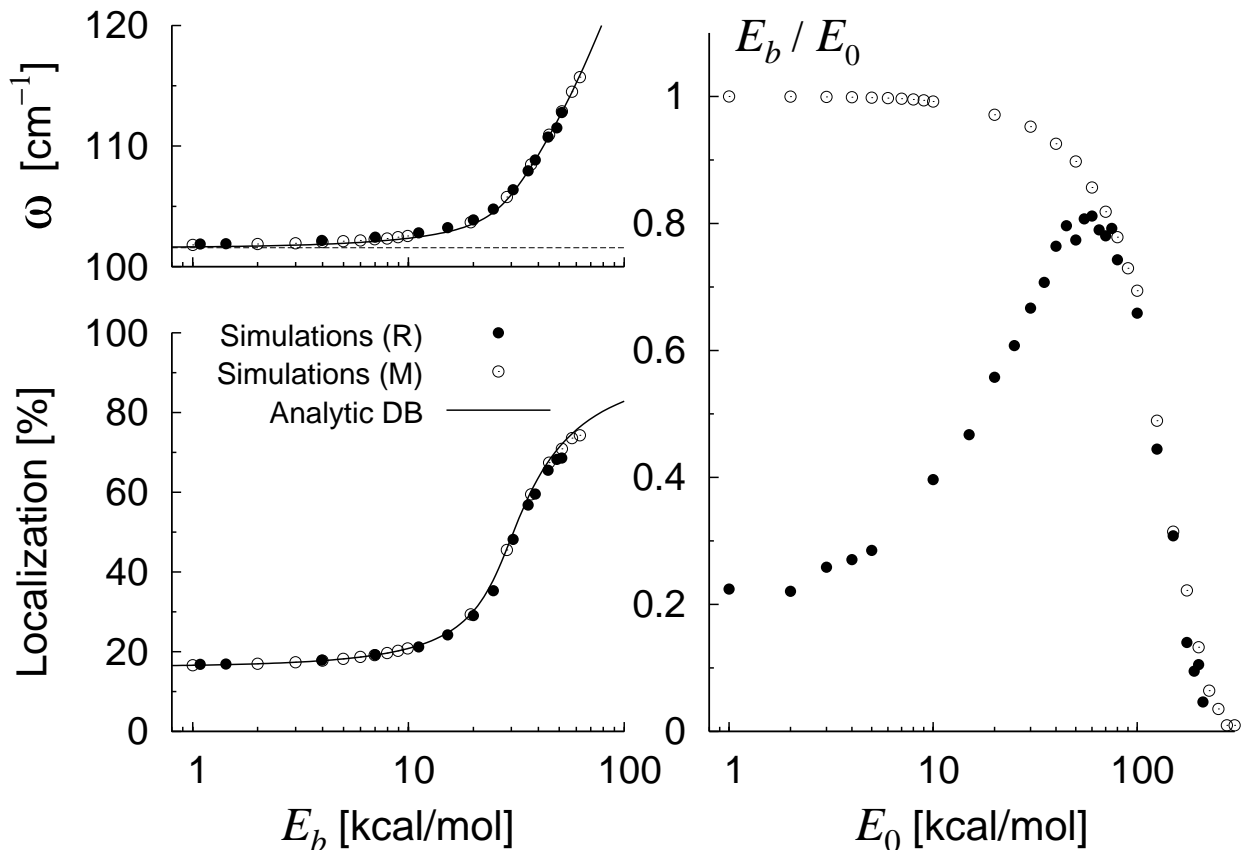


Figure 1: Local kicks cause energy pinning through the excitation of discrete breathers. The figure illustrates the formation of a discrete breather at site VAL 177 in subtilisin (PDB code 1AV7), a 274 amino-acids enzyme, following the excitation of the band-edge normal mode (M) or a single-site kinetic energy kick at VAL 177 (R), the residue where the edge NM is centered. The right panel reports the energy E_b found in the nonlinear localized mode as a function of the excitation energy E_0 . The left panels compare the frequency ω and the localization index L of the nonlinear mode with those of discrete breather solutions centered at VAL 177 calculated analytically, as described in ref. [1], showing that the nonlinear mode excited after a kick is indeed a discrete breather. The dashed line in the upper left plot marks the band-edge frequency of the protein network ($\omega_0 = 101.6$ cm⁻¹).

to spark the formation of a discrete breather, pinning a variable amount of energy E_b at a specific location. When less than 10 kcal/mole of kinetic energy is injected into the edge NM, nearly all this energy is kept by the DB, whose overlap with the edge NM is large at low energies. Increasing E_0 further, the frequency of the excited mode detaches from the linear band, while the excitation efficiency E_b/E_0 is eroded. In fact, as DB localization builds up with energy (see lower left panel), the spatial overlap with the edge NM diminishes, thus reducing excitation efficiency [4]. The same DB is also excited when the edge NM site is “kicked” along an *appropriate* direction, namely the maximum stiffness (MS) one [1] (see data marked (R) in Fig. 1). In this case, however, the excitation becomes more efficient as E_0 is increased, since the DB asymptotically approaches a single-site vibration. For $E_0 > 100$ kcal/mole, the DB loses its energy, which flows rapidly into the system.

B. Directional Specificity

We find that the maximum strain direction invariably allows for the most efficient excitation of a nonlinear mode at a given site. Fig. 2 illustrates the efficiency of kicks given along the MS direction, with respect to kicks imparted along random directions. The correlation with the squared cosine of the angle between the kick and the MS unit vectors indicates that it is the amount of energy injected along the MS vector which is the dominant factor allowing for efficient excitation of a discrete breather.

Interestingly, kicking away from the MS direction can promote energy transfer to another site. For instance, while a kick along the MS unit vector at the NM site of the band-edge mode invariably results in a DB sitting at the same site, when the direction of the kick is picked at random discrete breathers localized elsewhere are also observed (see again Fig. 2). In the following, we take advantage of the fact that MS directions can be

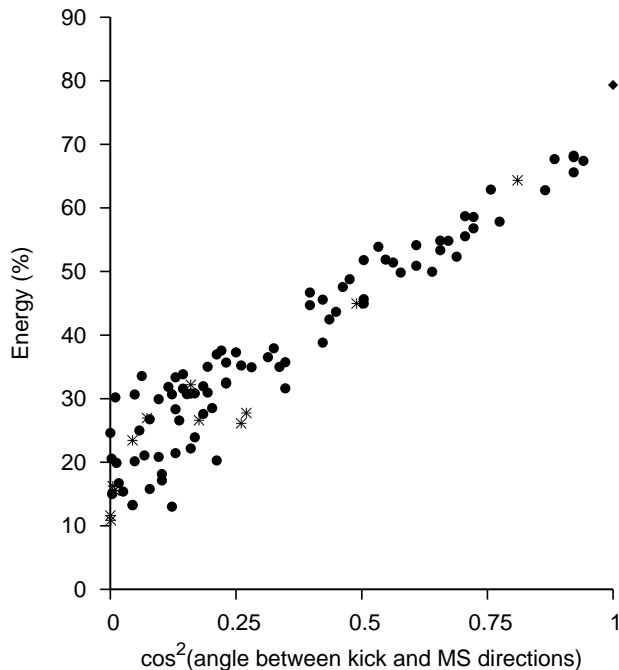


Figure 2: Optimum kick direction for exciting discrete breathers in dimeric citrate synthase (PDB code 1IXE). Percentage of the system energy found in a nonlinear mode as a function of the direction of the initial kick given to SER 213A, the NM site of the band-edge mode. The latter is measured by the angle θ between the kick direction and the MS unit vector. In all simulations, the (kinetic) energy of the kick is 55 kcal/mole and its direction is chosen at random, except when the maximum strain (MS) direction is picked instead (black diamond at $\cos\theta = 1$). Filled circles: SER 213A is found to be the most energetic site during the analysis timespan. Stars: it is another one. In one instance, while the kick was given in a direction close to the MS direction ($\cos\theta = 0.9$), the DB jumped on a neighboring site (namely, THR 208A).

easily calculated at any site in any structure [1] in order to investigate energy transfer in a systematic manner.

C. Energy Transfer

When a given residue is kicked along the MS direction, a transfer event can occur when $E_0 \gtrsim 20$ kcal/mol (see an example in Fig. 3). At peak transfer, more than 75 % of such kicks excite a DB localized at the band-edge NM site, while otherwise energy flows towards the NM site of another edge mode. Conversely, when the kick is imparted along a random direction, energy transfer is found to be less efficient.

Quite generally, a transfer event can be observed when almost any site is kicked, and in the majority of cases only a handful of well-defined sites are targeted. This means that energy transfer can occur between widely separated locations. Indeed, as illustrated in Fig. 4 for myosin, only about 5 % of 55 kcal/mole kicks result in a DB lo-

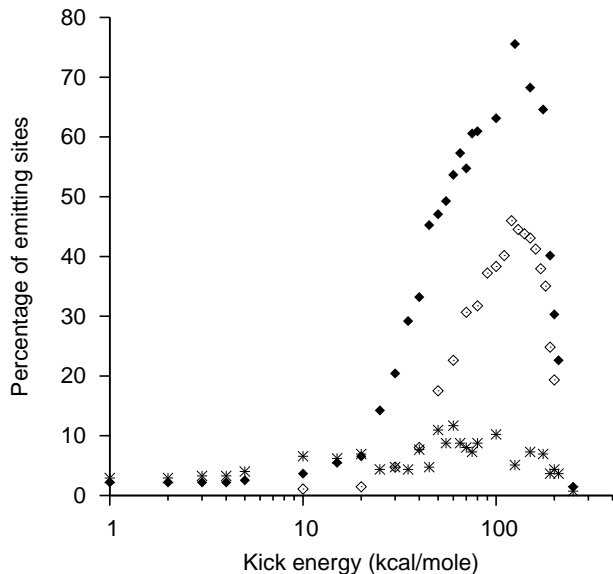


Figure 3: Energy transfer: all-site analysis. Percentage of sites in subtilisin that transmit most of the kick energy to the band-edge NM site, VAL 177 (black diamonds), or to the NM site of the second edge mode, MET 199 (stars). For a given kick energy, each site is kicked once, the most energetic nonlinear mode obtained is analyzed, and the site the most involved in this mode is recorded. When initial excitations are not imparted along the local stiffest direction, but are oriented at random, energy transfer towards VAL 177 is less likely (open diamonds).

calized at the same location. For all other kicked sites, a transfer occurs to a DB pinning a decreasing fraction of the excitation energy, one to eleven links away. Note that all high-yield and long-range energy transfers aim at the NM sites of one of the edge NMs, the NM site of the band-edge mode being the most likely target. Thus, energy systematically flows toward the stiffest regions of the structure. Interestingly, this is where functionally relevant residues tend to be located [1, 19, 26, 27, 28].

In one occurrence, more than 20% of the kick energy ends up in a nonlinear mode localized more than five links away: following a kick at TYR 34 a remarkable nine-link stretch is covered up to LEU 296, making a jump of more than 60 Å. However, cases of ultra long-range energy transfer like this are more rare and, at the same time, less efficient. In fact, as a consequence of the rather small amount of energy transferred (nearly 14 kcal/mole), the DB that self-excites at the target site is poorly localized (like in Fig. 1).

A more efficient transfer event, covering two links (about 11 Å), is analyzed in Fig. 5. At first, a DB is excited at the kicked site. However, due to interactions with the background, its energy slowly but steadily flows into the system. After approximately 1 ns, about 65 % of the excitation energy is still there. At $t = 1.1$ ns, this amount of energy is rapidly and almost entirely transferred to LEU 296, marking the self-localization of an-

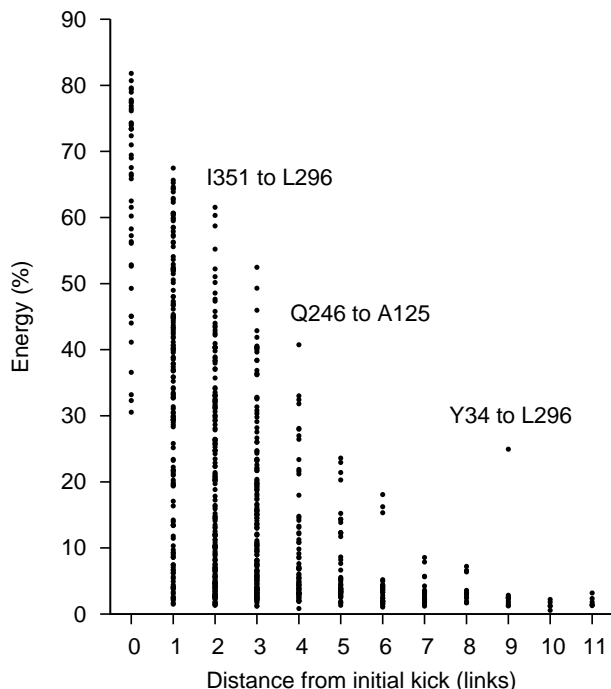


Figure 4: Energy transfer as a function of distance from excitation site. The figure illustrates the outcome of an all-site kick experiment in myosin, a large 746 amino-acids enzyme involved in muscle contraction (PDB code 1VOM). The fraction of excitation energy found in the DB is plotted versus the distance (in units of links in the connectivity graph) between the kicked site and the site where the nonlinear mode self-excites. The maximum amount of energy found in the DB decreases with the number of links separating the feed and the target sites. For instance, when GLN 246 is kicked, more than 40% of the energy ends up in a DB localized at ALA 125 (the band-edge NM site). This amounts to four links, corresponding to a span of about 25 Å in real space. Otherwise, when a kick is given to ILE 351, GLN 246 or TYR 34, 25-65% of the excitation energy flows either to ALA 125 or LEU 296, the NM site of the third edge normal mode. In cases where more than 30% of the kick energy is transferred away, three sites turn out to be targeted half of the times, namely ALA 125 (27%), LEU 296 (13%) and GLY 451 (7%). When only long-range energy transfers are considered (covering three or more links), the shares raise to 71 % and 18 % for ALA 125 and LEU 296, respectively. In the remaining cases, the DB is found either at LEU 516 (7%, 14th mode) or at ARG 80 (4%, 10th mode).

other DB. Although the transfer itself is a quite complex process, involving several intermediate sites, it may well prove to be an example of *targeted energy transfer* [14]. Indeed, as the energy of the DB at the the initial site drops, its frequency diminishes as well. This may allow for a transfer to occur if a resonance condition with the frequency of another DB is met. The transmission should be irreversible, as a consequence of both DBs' frequency drifts during energy exchange [14]. Note that, as the energy of the first DB is eroded, the mode becomes also less and less localized [1]. This, in turn, is likely to increase

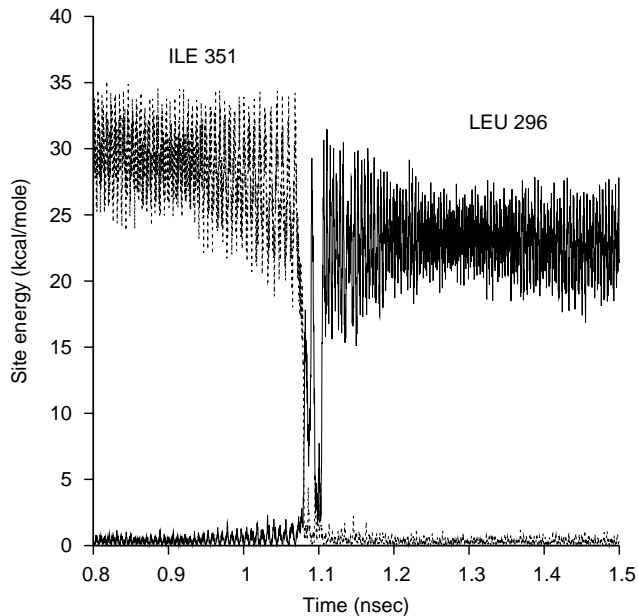


Figure 5: Site to site energy transfer in myosin. The local energies at sites ILE 351 (dotted line) and LEU 296 (solid line) are plotted as functions of time, after a 55 kcal/mole kick at ILE 351. The fluctuations occurring well before and after the transfer reflect the fact that the corresponding nonlinear modes are not perfectly localized on both sites. As a consequence, they exchange significant amounts of energy with their *environs*.

the overlap between the two DB displacement patterns, thus allowing for more efficient energy channelling [4, 8].

To gain further understanding on the transfer mechanism, we investigated energy circulation in a dimeric form of rhodopsin. Very few high-yield and long-range energy transfers were recorded between sites belonging to different monomers, the vast majority of transfer events being confined within the same domain. Indeed, in less than 1% of the instances more than 30% of the kick energy (55 kcal/mole) injected at one monomer is transmitted to the other. Here, at variance with most protein dimers, the stiffest regions are located in monomer bulks, so that the edge NMs are localized far away from the interface. This strongly suggests that energy transfers not only target stiff regions, but can couple any two sites efficiently only through rather stiff channeling pathways. On the other hand, when kicking one of the two (almost) equivalent sites of rhodopsin that are covalently linked to the retinal chromophore, up to about 50 % of the excitation energy ends up in a DB localized at one of three specific sites, the targeted location depending upon where (which monomer) the kick is imparted and on the magnitude of the latter. Interestingly, Fig. 6 reveals that transfer efficiency is optimum in the narrow range 50-55 kcal/mole, *i.e.* exactly the energy of photons that can be absorbed by the retinal chromophore when it is embedded within rhodopsin ($\lambda = 500 \div 550$ nm). Interestingly, the preferentially targeted residue in this energy range (GLU 113)

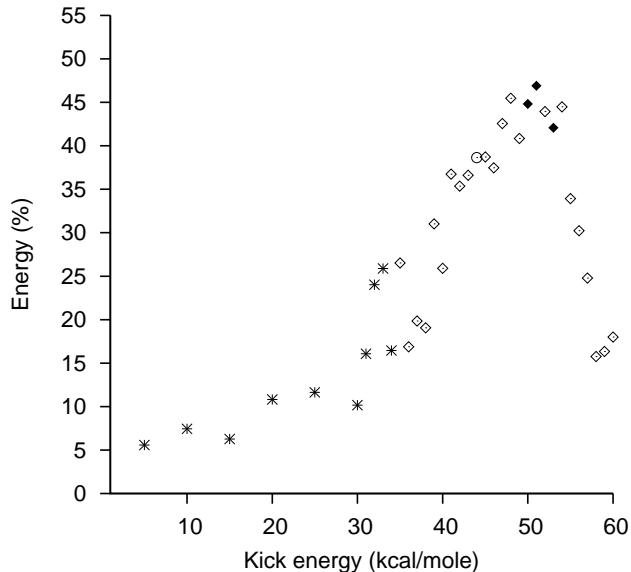


Figure 6: Energy transfer in rhodopsin (PDB code 3CAP). The fraction of energy E_b/E_0 found in the discrete breather when kicking the site attached to the retinal chromophore (LYS 296) of monomer B is plotted versus the excitation energy. Symbols indicate at which site the DB self-localizes: GLU 113 (black diamonds), CYS 185 (open diamonds), MET 86 (open circle) or another one (stars).

is known to be involved in the early stages of the signaling cascade following rhodopsin activation [29].

III. DISCUSSION

In summary, despite its coarse-grained nature, the NNM framework is able to provide biologically sensible clues about energy circulation in proteins. High-yield and long-range energy transfers systematically pin energy at the sites the most involved in a small subset of band-edge linear modes, that is, within the stiffest parts of protein structures. These, in turn, are the regions preferentially hosting residues involved in catalytic mechanisms [1, 19, 26, 27, 28]. Thus, what our study suggests is that protein structures may have been designed, during the course of evolution, so as to allow energy to flow where it is needed, *e.g.* to, or close to catalytic sites, with the aim of lowering the energy barriers that have to be overcome during catalytic processes.

Interestingly, in view of the coarse-grained nature of the NNM scheme, the same site-specific, high-yield and long-range energy transfers observed in proteins are also likely to occur in other physical systems, possibly simpler to engineer and to handle, so long as they share with

proteins both spatial and stiffness heterogeneity.

IV. METHODS

Proteins are modelled as networks of nodes of mass M (the α -carbons of their amino-acid residues) linked by springs. Specifically, in the nonlinear network model (NNM) [1, 19], the potential energy of a protein, E_p , has the following form:

$$E_p = \sum_{d_{ij}^0 < R_c} \left[\frac{k_2}{2} (d_{ij} - d_{ij}^0)^2 + \frac{k_4}{4} (d_{ij} - d_{ij}^0)^4 \right]$$

where d_{ij} is the distance between particles i and j , d_{ij}^0 their distance in the equilibrium structure (as *e.g.* solved through X-ray crystallography) and R_c is a distance cut-off that specifies which pairs of nodes are interacting. Note that $k_4 = 0$ corresponds to the widely used Elastic Network Model (ENM) [30, 31, 32], which has proven useful for quantitatively describing amino-acid fluctuations at room temperature [30, 31, 33], as well as for predicting and characterizing large-amplitude functional motions of proteins [34, 35, 36, 37, 38], in agreement with all-atom models [39, 40, 41], paving the way for numerous applications in structural biology [42], such as fitting atomic structures into low-resolution electron density maps [43, 44], or providing templates for molecular replacement techniques [45]. As in previous NNM studies [1, 19], we take $R_c = 10 \text{ \AA}$, $k_4 = 5 \text{ kcal/mol/\AA}^4$ and fix k_2 so that the low-frequency part of the linear spectrum matches actual protein frequencies, as calculated using realistic force fields [42]. When $M = 110 \text{ a.m.u.}$ (the average amino-acid residue mass), this gives $k_2 = 5 \text{ kcal/mol/\AA}^2$.

For each site in a given structure, the maximum-stiffness (MS) direction is computed through the Sequential Maximum Strain algorithm [1]. Following an initial kinetic-energy impulse (kick) at a specific site along the local MS unit vector, a 2-ns microcanonical simulation is performed. After a 1-ns transient period during which a part of the excitation energy flows into the system, the velocity-covariance matrix is computed. Its first eigenvector provides the pattern of correlated site velocities involved in the dominant (most energetic) nonlinear mode (the DB). Accordingly, a transfer is recorded to the site at which the first principal mode (PM1) is found localized. Projecting the system trajectory on PM1 yields fair estimates of the DB frequency and average energy [19]. The localization index L of a DB centered at site m is obtained from the weight of the latter in the normalized displacement pattern of the DB, namely $L = 100 \times \sum_{\alpha=x,y,z} [\xi_\alpha(m)]^2$, where $\xi_\alpha(m)$ are the components at site m of PM1.

[1] Piazza, F, Sanejouand, YH (2008) Discrete breathers in protein structures. *Phys. Biol* 5:026001.

[2] Karplus, M, Kuriyan, J (2005) Molecular dynamics and

- protein function. *Proc. Natl. Acad. Sci. USA* 102:6679–6685.
- [3] Levy, R, Perahia, D, Karplus, M (1982) Molecular dynamics of an alpha-helical polypeptide: temperature dependence and deviation from harmonic behavior. *Proc. Natl. Acad. Sci. USA* 79:1346–1350.
- [4] Moritsugu, K, Miyashita, O, Kidera, A (2000) Vibrational energy transfer in a protein molecule. *Phys. Rev. Letters* 85:3970–3973.
- [5] Sagnella, D, Straub, J, Thirumalai, D (2000) Time scales and pathways for kinetic energy relaxation in solvated proteins: Application to carbonmonoxy myoglobin. *J. Chem. Phys.* 113:7702–7711.
- [6] Hennig, D (2002) Energy transport in alpha-helical protein models: One-strand versus three-strand systems. *Phys. Rev. B* 65.
- [7] Ishikura, T, Yamato, T (2006) Energy transfer pathways relevant for long-range intramolecular signaling of photosensory protein revealed by microscopic energy conductivity analysis. *Chemical Physics Letters* 432:533–537.
- [8] Leitner, DM (2008) Energy flow in proteins. *Annual Review of Physical Chemistry* 59:233–259.
- [9] Davydov, A (1977) Solitons and energy transfer along protein molecules. *J. Theor. Biol.* 66:379–387.
- [10] Peyrard, M (1995) *Nonlinear excitations in biomolecules* (Springer, Berlin).
- [11] Dauxois, T, Litvak-Hinenzon, A, MacKay, R, Spanoudaki, A, eds (2004) *Energy localisation and transfer in crystals, biomolecules and josephson arrays. Advanced Series in Nonlinear Dynamics, vol.22* (World Scientific, Singapore).
- [12] Mingaleev, SF, Christiansen, PL, Gaididei, YB, Johansson, M, Rasmussen, KØ (1999) Models for energy and charge transport and storage in biomolecules. *Journal of Biological Physics* 25:41–63.
- [13] d’Ovidio, F, Bohr, HG, Lindgard, PA (2005) Analytical tools for solitons and periodic waves corresponding to phonons on lennard-jones lattices in helical proteins. *Physical Review E* 71:026606.
- [14] Kopidakis, G, Aubry, S, Tsironis, GP (2001) Targeted energy transfer through discrete breathers in nonlinear systems. *Phys. Rev. Lett.* 87:165501.
- [15] Archilla, JFR, Gaididei, YB, Christiansen, PL, Cuevas, J (2002) Stationary and moving breathers in a simplified model of curved alpha-helix proteins. *Journal of Physics A* 35:8885–8902.
- [16] Flach, S, Gorbach, AV (2008) Discrete breathers – advances in theory and applications. *Physics Reports* 467:1–116.
- [17] Sato, M, Sievers, A (2009) Experimental and numerical exploration of intrinsic localized modes in an atomic lattice. *Journal of Biological Physics* 35:57–72.
- [18] Flach, S, Willis, CR (1998) Discrete breathers. *Phys. Rep.* 295:181–264.
- [19] Juanico, B, Sanejouand, YH, Piazza, F, De Los Rios, P (2007) Discrete breathers in nonlinear network models of proteins. *Phys. Rev. Lett.* 99:238104.
- [20] Livi, R, Franzosi, R, Oppo, GL (2006) Self-localization of bose-einstein condensates in optical lattices via boundary dissipation. *Physical Review Letters* 97:060401–4.
- [21] Piazza, F, Lepri, S, Livi, R (2003) Cooling nonlinear lattices toward energy localization. *Chaos* 13:637–645.
- [22] Reigada, R, Sarmiento, A, Lindenberg, K (2001) Energy relaxation in nonlinear one-dimensional lattices. *Physical Review E* 64.
- [23] Dauxois, T, Khomeriki, R, Piazza, F, Ruffo, S (2005) The anti-fpu problem. *Chaos* 15:015110.
- [24] Cretegny, T, Dauxois, T, Ruffo, S, Torcini, A (1998) Localization and equipartition of energy in the [beta]-fpu chain: Chaotic breathers. *Physica D: Nonlinear Phenomena* 121:109–126.
- [25] Sitnitsky, A (2006) Dynamical contribution into enzyme catalytic efficiency. *Physica A: Statistical Mechanics and its Applications* 371:481–491.
- [26] Yang, L, Bahar, I (2005) Coupling between catalytic site and collective dynamics: a requirement for mechanochemical activity of enzymes. *Structure* 13:893–904.
- [27] Sacquin-Mora, S, Laforet, E, Lavery, R (2007) Locating the active sites of enzymes using mechanical properties. *Proteins* 67:350–359.
- [28] Haliloglu, T, Erman, B (2009) Analysis of Correlations between Energy and Residue Fluctuations in Native Proteins and Determination of Specific Sites for Binding. *Physical Review Letters* 102:088103.
- [29] Yan, E et al. (2003) Retinal counterion switch in the photoactivation of the g protein-coupled receptor rhodopsin. *Proc. Natl. Acad. Sci. USA* 100:9262–9267.
- [30] Tirion, M (1996) Low-amplitude elastic motions in proteins from a single-parameter atomic analysis. *Phys. Rev. Lett.* 77:1905–1908.
- [31] Bahar, I, Atilgan, AR, Erman, B (1997) Direct evaluation of thermal fluctuations in proteins using a single-parameter harmonic potential. *Fold. Des.* 2:173–181.
- [32] Hinsen, K (1998) Analysis of domain motions by approximate normal mode calculations. *Proteins* 33:417–429.
- [33] Kondrashov, D, Van Wynsberghe, A, Bannen, R, Cui, Q, Phillips, G (2007) Protein structural variation in computational models and crystallographic data. *Structure* 15:169–177.
- [34] Tama, F, Sanejouand, YH (2001) Conformational change of proteins arising from normal mode calculations. *Prot. Eng.* 14:1–6.
- [35] Delarue, M, Sanejouand, YH (2002) Simplified normal modes analysis of conformational transitions in dna-dependant polymerases: the elastic network model. *J. Mol. Biol.* 320:1011–1024.
- [36] Krebs, WG et al. (2002) Normal mode analysis of macromolecular motions in a database framework: developing mode concentration as a useful classifying statistic. *Proteins* 48:682–695.
- [37] Lu, M, Ma, J (2005) The Role of Shape in Determining Molecular Motions. *Biophys. J.* 89:2395–2401.
- [38] Nicolay, S, Sanejouand, YH (2006) Functional modes of proteins are among the most robust. *Phys. Rev. Lett.* 96:078104.
- [39] McCammon, JA, Gelin, BR, Karplus, M, Wolynes, P (1976) The hinge-bending mode in lysozyme. *Nature* 262:325–326.
- [40] Marques, O, Sanejouand, YH (1995) Hinge-bending motion in citrate synthase arising from normal mode calculations. *Proteins* 23:557–560.
- [41] Perahia, D, Mouawad, L (1995) Computation of low-frequency normal modes in macromolecules: improvements to the method of diagonalization in a mixed basis and application to hemoglobin. *Comput. Chem.* 19:241–246.
- [42] Bahar, I, Cui, Q, eds (2005) *Normal Mode Analysis: The-*

ory and Applications to Biological and Chemical Systems. *C&H/CRC Mathematical & Computational Biology Series, vol. 9* (CRC press, Boca Raton).

- [43] Tama, F, Miyashita, O, Brooks III, CL (2004) Flexible multi-scale fitting of atomic structures into low-resolution electron density maps with elastic network normal mode analysis. *J. Mol. Biol.* 337:985–999.
- [44] Delarue, M, Dumas, P (2004) On the use of low-frequency normal modes to enforce collective movements in refining macromolecular structural models. *Proc. Natl. Acad. Sci. USA* 101:6957–6962.
- [45] Suhre, K, Sanejouand, YH (2004) On the potential of normal mode analysis for solving difficult molecular replacement problems. *Act. Cryst. D* 60:796–799.